

Common-Reflection-Surface stack for converted waves

S. Bergler, E. Duveneck, G. Höcht, Y. Zhang, and P. Hubral

email: *Steffen.Bergler@gpi.uni-karlsruhe.de*

keywords: *wavefield separation, CRS attributes*

ABSTRACT

The finite-offset (FO) common-reflection-surface (CRS) stack has been shown to be able to handle P-P, S-S and also P-S or S-P converted reflections to provide different stack sections such as common-offset (CO), common-midpoint (CMP) and common-shot (CS) sections from the multi-coverage pre-stack seismic data in a data-driven (model independent) way. It is our purpose in this paper to investigate the performance of the FO CRS stack on data involving converted waves in inhomogeneous layered media. We accomplish this by applying the FO CRS stack for common-offset to a synthetic seismic data set involving P-P as well as P-S converted primary reflections. We demonstrate that the FO CRS stack yields convincing improvement of the image quality in the presence of noisy data and successfully extracts kinematic wavefield attributes useful for further analyzes. The extracted emergence angle information is used to achieve a complete separation of the wavefield into its P-P and P-S wave components, given the FO CRS stacked horizontal and vertical component sections.

INTRODUCTION

To find a successful coherency-based stacking technique to enhance P-S or S-P reflections in pre-stack (multi-coverage) seismic data as, for instance, by a common-midpoint (CMP) or common-conversion point (Tessmer and Behle, 1990; Tessmer et al., 1990; Iverson et al., 1989) stack is a more difficult task than to stack P-P or S-S reflections. Together with performing an optimal stack one desires, of course, to extract from the P-P (or S-S) and P-S (or S-P) reflection data the moveout parameters, which depend on the specific gathers as, e.g., the CMP or common-reflection-point (CRP) gathers. The coherency-based data-derived moveout parameters may then be used to separate different wave types, or to determine in a subsequent travelt ime inversion the v_p (P-wave velocity) and/or v_s (S-wave velocity) of a layered earth model.

With the introduction of the POLYSTACK (de Bazelaire, 1988), Multifocusing (Gelchinsky, 1989), and the Common-Reflection-Surface (CRS) stack (Jäger et al., 2001) three-parameter moveout surfaces rather than one- or two-parameter moveout trajectories were introduced to stack P-P reflections in 2-D pre-stack data into a simulated zero-offset section. These moveout

surfaces depend on the near-surface velocity and the midpoint and offset coordinates (Hubral, 1999). To handle also converted reflections in the frame of the CRS stack, the ZO CRS stack has recently been generalized to stack pre-stack data into a selected finite-offset (FO) section (Zhang et al., 2001). In this case the moveout surfaces are described by five parameters, which have to be searched-for in a coherency-based, data-driven (model independent) way. If the selected FO section is a common-offset (CO) section, we refer to this method as CO CRS stack (Bergler et al., 2001).

In this paper the problem is the following: Given a two-component registration (synthetic data) of P-P and P-S reflections on a seismic line, we want to extract from noisy multi-coverage pre-stack data a well enhanced P-P as well as a P-S finite-offset section by means of the CO CRS stack. Our results demonstrate the convincing advantage of the CO CRS stack over conventional stacks in improving the imaging quality, in the presence of a low signal-to-noise ratio, at the same time allowing a complete separation of P-P and P-S reflections. In future it is planned to apply this technique to real data.

BASIC THEORY

To handle converted reflections in the frame of the CO CRS stack, we make use of a five-parameter moveout formula (Zhang et al., 2001). It reads

$$T^2 = \left(t_0 + \frac{\sin \beta_G}{v_G} \Delta x_G - \frac{\sin \beta_S}{v_S} \Delta x_S \right)^2 + 2t_0 \left(-\Delta x_S B^{-1} \Delta x_G + \frac{1}{2} \Delta x_S B^{-1} A \Delta x_S + \frac{1}{2} \Delta x_G D B^{-1} \Delta x_G \right), \quad (1)$$

where t_0 is the travelttime along the central ray. Δx_S and Δx_G are the lateral displacement of the paraxial ray with respect to the central ray at the source and receiver, respectively. In the work of Červený (2001), the equation is presented in a different form and is called the two-point eikonal. If we define the increment of the midpoint and the increment of the half-offset as

$$\Delta x_m = \frac{1}{2}(\Delta x_G + \Delta x_S) \quad \text{and} \quad \Delta h = \frac{1}{2}(\Delta x_G - \Delta x_S), \quad (2)$$

we can alter equation (1) into the moveout formula in terms of midpoint and half-offset

$$T^2 = \left[t_0 + \left(\frac{\sin \beta_G}{v_G} - \frac{\sin \beta_S}{v_S} \right) \Delta x_m + \left(\frac{\sin \beta_G}{v_G} + \frac{\sin \beta_S}{v_S} \right) \Delta h \right]^2 + 2t_0 \left[\Delta x_m (D B^{-1} - B^{-1} A) \Delta h + \frac{1}{2} \Delta x_m (B^{-1} A + D B^{-1} - 2B^{-1}) \Delta x_m + \frac{1}{2} \Delta h (B^{-1} A + D B^{-1} + 2B^{-1}) \Delta h \right]. \quad (3)$$

In both equations (1) and (3) the parameters β_S and β_G are the incidence angle and the emergence angle of the central ray at the source and the receiver, respectively, v_S and v_G are the wave velocities at the source and at the receiver, respectively. The quantities A , B , and D in the equations

are the scalar elements of the surface-to-surface ray propagator matrix given by Bortfeld (1989)

$$\underline{\mathbf{T}} = \begin{pmatrix} A & B \\ C & D \end{pmatrix}, \quad (4)$$

of a fixed central ray, which possesses the symplectic property (Červený, 2001)

$$AD - BC = 1. \quad (5)$$

For every sample of the finite-offset section to be reconstructed, we need to determine the moveout surface, defined by five parameters β_S , β_G , A , B , and D , that best fits the pre-stack reflections. We do that by means of searches in the multi-coverage data volume, using coherency analysis, e.g., semblance (Taner and Koehler, 1969). In the upper part of figure 1 two five-parameter moveout surfaces (or CRS stacking surfaces) are shown for two particular stack output samples (for P-P and P-S indicated by arrows) in the midpoint-half-offset-traveltime pre-stack data volume. The moveout surfaces—depicted for one P-P and one P-S reflection—approximate the kinematic reflection responses of the P-P and P-S reflections from the dome-like interface in the vicinity of the respective output samples. The model is shown on the front-side of the lower part in figure 1. The two output samples are associated with the two P-P and P-S reflected rays in this 2-D laterally inhomogeneous medium. If the horizontal and vertical-component geophone registrations along the seismic line are available, we have two kinematically identical multi-coverage data sets but with different amplitudes. Once the CRS stacking surfaces are determined from the data for every stack output sample of an a priori specified finite-offset section, the CRS stack along these surfaces can be carried out to get two CO CRS stack sections, one for each recorded component. In this way, we make use of the full two-component multi-coverage data volume. In one of the two obtained sections a P-P reflection event will be easier to identify than a P-S reflection and vice versa. For various strategies of performing an accurate and efficient parameter search and for uses of the five data-derived kinematic wave field attributes we want to refer to Zhang et al. (2001). The inline geometrical spreading factor can, for instance, be computed from the attributes (Zhang et al., 2001), which is of help for AVO analysis.

SEPARATION OF CONVERTED AND NON-CONVERTED WAVES

To actually separate P-P and P-S reflections the emergence angle section β_G , which is an additional output of the CO CRS stack, can be used. It gives the ray direction of emerging P- or S-waves, depending on the velocity used for v_G in equation (3) (in fact $\sin \beta_G/v_G$ is determined during the search (see Bergler et al., 2001) and β_G can be calculated for any choice of v_G corresponding to the near-surface P- or S-wave velocity afterwards).

Assume an entire angle section β_G , calculated using the near-surface propagation velocity of P-waves. The direction of the ray at the receiver, given by β_G defines the polarization direction of a P-wave traveling along this ray at the same position (tangential to the ray, if free-surface effects are neglected and an isotropic near-surface velocity is assumed). At the same time the polarization direction defined by the relative amplitudes of the horizontal and vertical components can be calculated directly from the two corresponding CO CRS stack sections. If a given

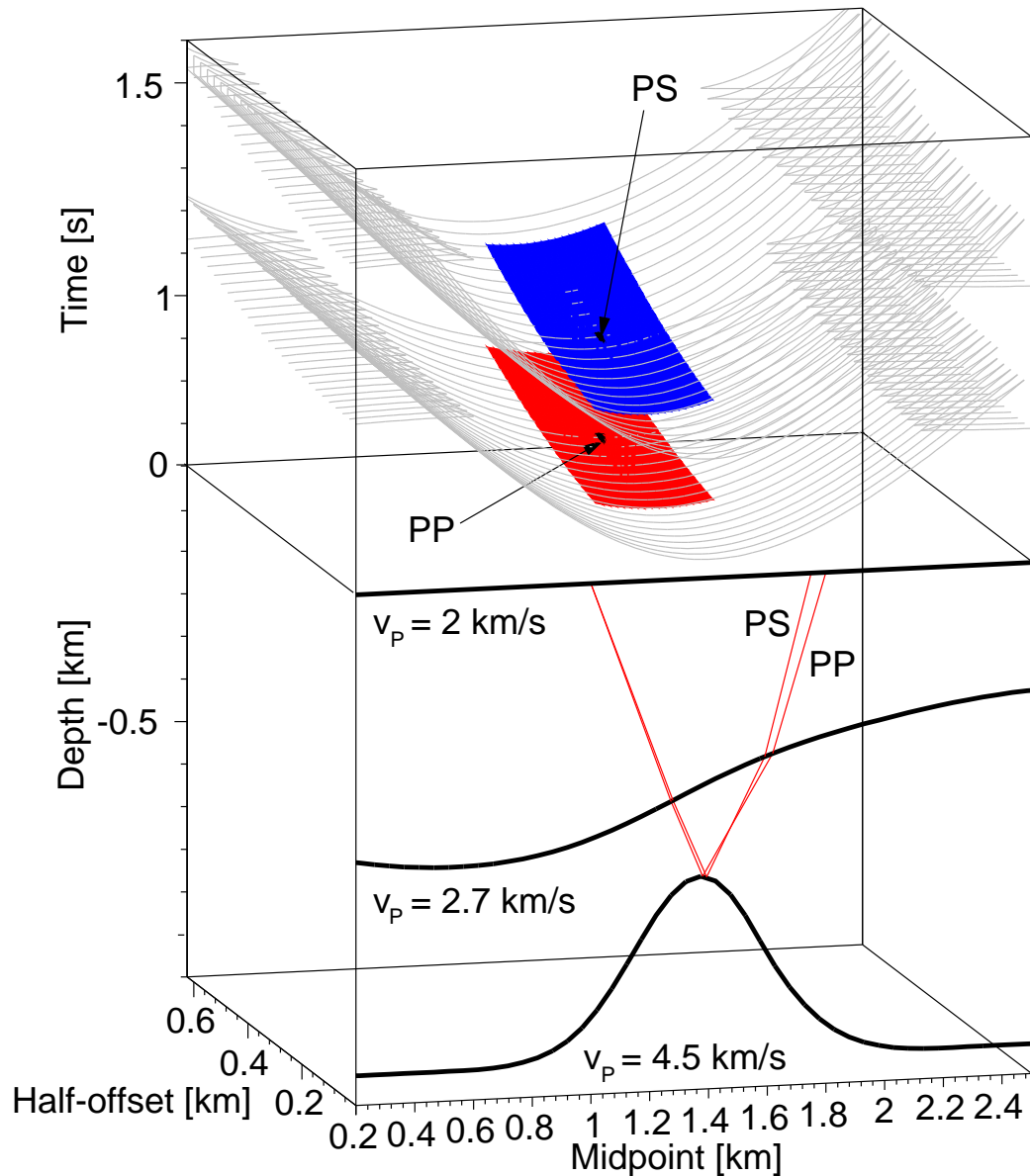


Figure 1: Upper part: The kinematic reflection response of P-P and P-S waves (grey curves) from the dome-like interface are depicted in the midpoint–half-offset–traveltime volume. At two stack output samples the kinematic reflection response is approximated by the corresponding CRS stacking surface which are found by coherency analysis. Lower part: The two rays associated with the two stack output samples are depicted.

event stems from an emerging P-wave, the polarization calculated directly from the two components and the polarization defined by the ray emergence direction should coincide, while for an emerging S-wave they should deviate significantly.

We denote the angle between the directly measured polarization and the polarization defined by the direction of the emerging ray by γ . It serves as a criterion to distinguish P- and S-waves. A weight function $w(\gamma)$ that suppresses events with large γ and preserves events with γ close to zero can then be applied to the amplitude computed from horizontal and vertical components. Such a function could, for example, be of the form $w(\gamma) = \cos^{2n+1} \gamma$ where $n > 0$ is an arbitrary integer. A simple projection ($n = 0$) onto the ray tangent direction would not suffice to completely suppress S-waves, because their polarization direction will not be exactly normal to the ray direction, which was determined assuming P-wave velocity for v_G .

An analogous procedure can be applied to enhance S-waves. In that case the angle section β_G obtained by the CO CRS stack is calculated using the near-surface propagation velocity of an S-wave. The expected polarization direction of an S-wave traveling along that ray would then be normal to the ray direction.

RESULTS ON SYNTHETIC DATA

For the 2-D medium shown in the lower part of Figure 1 we generated two synthetic multi-coverage data sets, where the horizontal as well as the vertical component seismograms were registered. For simplicity free-surface effects have been neglected. For the generation of the pre-stack data we considered only primary P-P and P-S reflections from the two interfaces for half-offsets from 0 km to 0.625 km in increments of 0.025 km. Thus, we have a maximum fold of 26. The midpoints ranged between 0.2 km and 2.5 km with an interval of 0.025 km. As seismic signal we used a zero-phase Ricker wavelet of 30 Hz peak-frequency. The sampling interval was 4 ms. The S-wave velocities of the three layers were defined by the constant $v_p/v_s = \sqrt{3}$ ratio. Finally, random noise was added to the traces so that every CO section looks similar to those shown in Figures 2(a) and 2(b) with respect to the signal-to-noise ratio. Figure 2(a) shows a CO section of the noisy vertical-component registration and Figure 2(b) a CO section of the noisy horizontal-component registration. The half-offset for both sections is 0.5 km. Both CO sections were then constructed from the pre-stack data by the CRS stack for finite-offsets. The CRS stack for the vertical component is shown in Figure 3(a) and for the horizontal component in Figure 3(b). In both CRS stack sections the signal-to-noise ratio increased more than in the corresponding CMP stacks (not shown). In the CMP stack only the two-parameter CMP stacking trajectories confined to the CMP gathers were used instead of the five-parameter CRS moveout surfaces.

Next a wavefield separation as described in the previous section was performed. In this case a weight function $w(\gamma) = \cos^5 \gamma$ was applied to the amplitudes computed from the vertical and horizontal component CRS stack sections. As can be seen in Figure 4(a) (P-P reflections) and Figure 4(b) (P-S reflections), a complete separation is achieved.

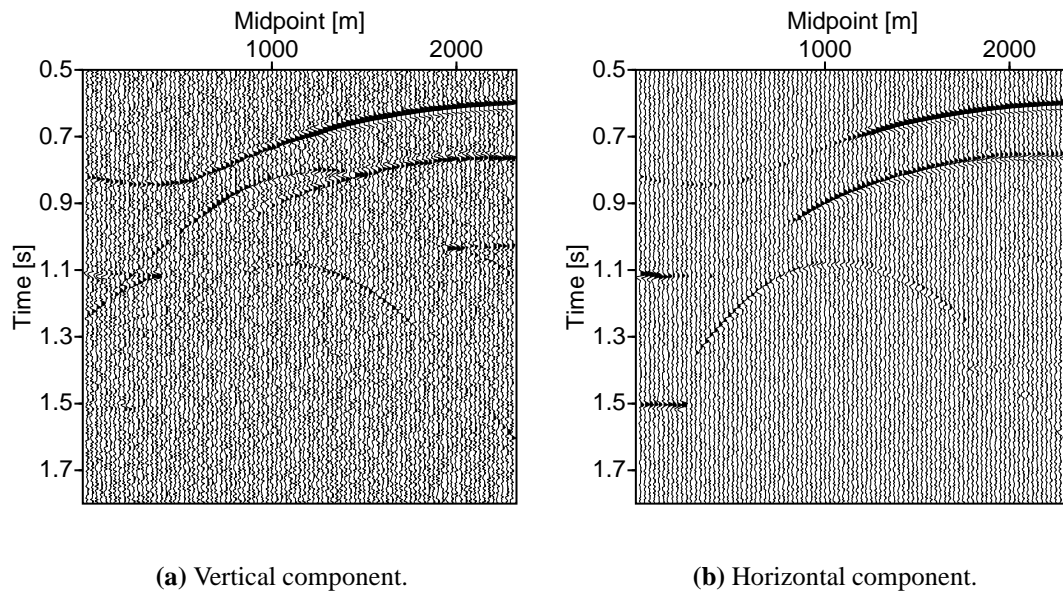


Figure 2: CO sections of pre-stack data set.

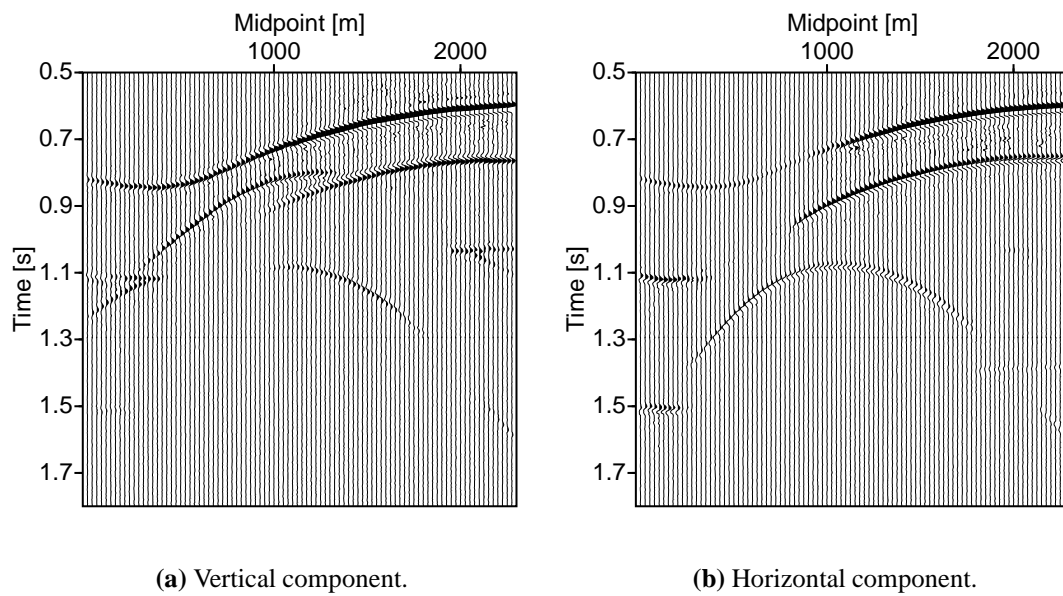


Figure 3: CRS stacked CO sections.

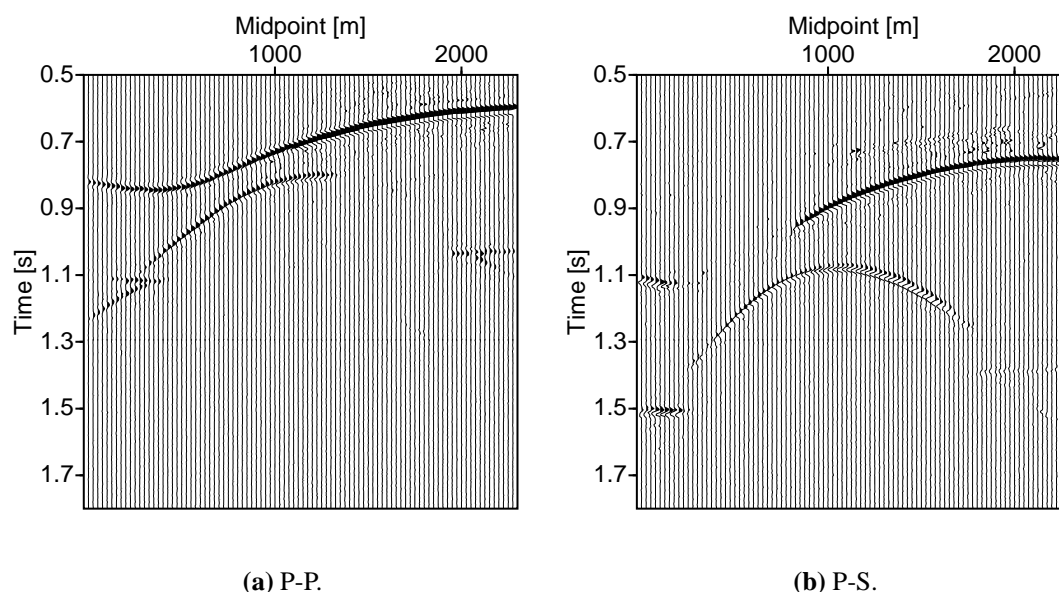


Figure 4: Reflections extracted from CRS stacked CO sections.

CONCLUSIONS

We demonstrated the applicability of the new Common-Offset (CO) CRS stack to seismic multi-coverage data containing converted reflections. Our results on synthetic multi-component data indicate that the CO CRS stack on converted reflections may prove on real data to be an attractive alternative to conventional stacking methods. With the need of nothing more than the near-surface velocity, the purely data-driven five-parameter CO CRS stack yields convincing imaging results in the example considered in this paper. When applied to multi-component data the emergence angle information provided by the CO CRS stack can be used to reliably separate P-P from P-S reflections. The significantly improved signal-to-noise ratio on both, the horizontal and vertical component sections and the ability to obtain separate P-P and P-S sections show the great potential of the CO CRS stack in the processing and interpretation of converted waves. This will be further investigated on real data involving converted waves, where also the five kinematic wave field attributes will be considered for further use in inversion (e.g. macro-model inversion, AVO analysis, etc).

REFERENCES

- Bergler, S., Höcht, G., Zhang, Y., and Hubral, P. (2001). Common-Reflection-Surface stack for common-offset: practical aspects. In *Extended Abstracts*. 63th Mtg. Eur. Assn. Geosci. Eng. Session P 076.
- Bortfeld, R. (1989). Geometrical ray theory: Rays and traveltimes in seismic systems (second-order approximations of the traveltimes). *Geophysics*, 54(3):342–349.

- Červený, V. (2001). *Seismic Ray Theory*. Cambridge University Press.
- de Bazelaire, E. (1988). Normal moveout revisited - inhomogeneous media and curved interfaces. *Geophysics*, 53(2):143–157.
- Gelchinsky, B. (1989). Homeomorphic imaging in processing and interpretation of seismic data - fundamentals and schemes. In *59th Ann. Internat. Mtg*, page 983. Soc. Of Expl. Geophys.
- Hubral, P., editor (1999). *Macro-model independent seismic reflection imaging*, volume 42. J. Appl. Geophys.
- Iverson, W. P., Fahmy, B. A., and Smithson, S. B. (1989). VpVs from mode-converted P-SV reflections. *Geophysics*, 54(07):843–852.
- Jäger, R., Mann, J., Höcht, G., and Hubral, P. (2001). Common-reflection-surface stack: Image and attributes. *Geophysics*, 66(1):97–109.
- Taner, M. T. and Koehler, F. (1969). Velocity spectra – digital computer derivation and applications of velocity functions. *Geophysics*, 34(6):859–881.
- Tessmer, G. and Behle, A. (1990). *Common reflection point data-stacking technique for converted waves*, pages 328–345. Soc. Of Expl. Geophys.
- Tessmer, G., Krajewski, P., Fertig, J., and Behle, A. (1990). Processing of PS-reflection data applying a common conversion-point stacking technique. *Geophys. Prosp.*, 38(03):267–286.
- Zhang, Y., Bergler, S., and Hubral, P. (2001). Common-Reflection-Surface (CRS) stack for common-offset. *Geophys. Prosp.*, 49(6):709–718.